JOURNAL OF GEOPHYSICAL RESEARCH, VOL. 111, D21115, doi:10.1029/2005JD006488, 2006

Gas age–ice age differences and the chronology of the Vostok ice core, 0–100 ka

M. L. Bender,[1] G. Floch,[2] J. Chappellaz,[3] M. Suwa,[1] J.-M. Barnola,[3] T. Blunier,[2] G. Dreyfus,[1,4] J. Jouzel,[4] and F. Parrenin[3]

Received 13 July 2005; revised 30 March 2006; accepted 17 July 2006; published 14 November 2006.

[1] Gas is trapped in polar ice at depths of ~50–120 m and is therefore significantly younger than the ice in which it is embedded. The age difference is not well constrained for slowly accumulating ice on the East Antarctic Plateau, introducing a significant uncertainty into chronologies of the oldest deep ice cores (Vostok, Dome Fuji, and Dome C). We recorrelate the gas records of Vostok and Greenland Ice Sheet Project 2 (GISP2) cores in part on the basis of new CH_4 data and use these records to construct six Vostok chronologies that use different assumptions to calculate gas age–ice age differences. We then evaluate these chronologies by comparing times of climate events at Vostok with correlative events in the well-dated Byrd ice core (West Antarctica). From this evaluation we identify two leading chronologies for the Vostok core that are based on recent models of firn temperature, firn densification, and thinning of upstream ice. One chronology involves calculating gas age–ice age differences from these models. The second, new, approach involves calculating ice depths in the core that are contemporaneous with depths in the same ice core whose gas ages are well constrained. This latter approach circumvents problems associated with highly uncertain accumulation rates in the Vostok core. The uncertainty in Vostok chronologies derived by correlating into the GISP2 gas record remains about ±1 kyr, and high-precision correlations continue to be difficult.

Citation: Bender, M. L., G. Floch, J. Chappellaz, M. Suwa, J.-M. Barnola, T. Blunier, G. Dreyfus, J. Jouzel, and F. Parrenin (2006), Gas age–ice age differences and the chronology of the Vostok ice core, 0–100 ka, *J. Geophys. Res.*, *111*, D21115, doi:10.1029/2005JD006488.

1. Introduction

[2] Ice cores record environmentally significant properties both in the gas phase and the ice phase. Properties recorded in the ice include aerosols content and the isotopic composition of precipitation. Properties registered in the gas phase include the concentration and isotopic composition of biogenic greenhouse gases. Gases are trapped ~50–120 m below the surface, where the ice is compressed to a density of about 0.82 gm cm^{-3} (density of pure ice = 0.917). Firn is openly porous and permeable down to the trapping depth. Air mixes rapidly to this depth, and trapped air is younger than the enclosing ice.

[3] Examining the timing of environmental changes recorded in ice and in trapped gas requires correcting for the age difference in the two phases. In the case of slowly accumulating East Antarctic ice cores, this difference is very large, up to 7 kyr during glacial periods, and the timing of climate changes recorded in the two phases will not be accurate unless the gas age–ice age difference can be well constrained. The gas age–ice age difference (Δage) is usually computed from estimates of surface temperature, accumulation rate, and an empirical or mechanistic model that expresses close-off depth and Δage in terms of these properties [e.g., *Herron and Langway*, 1980]. This approach works very well in high-accumulation-rate sites where it has been tested, notably in central Greenland [*Goujon et al.*, 2003]. However, there is a problem concerning East Antarctica. A property of firn related to the close-off depth is registered in the $\delta^{15}N$ of trapped N_2. The registration mechanism is gravitational fractionation, which causes heavy isotopes and gases to be enriched at a specified rate with depth [*Craig et al.*, 1988; *Schwander*, 1989; *Sowers et al.*, 1989] (Figure 1). The problem is that the ^{15}N enrichment in glacial samples is up to 1/3 less than predicted by the empirical and mechanistic models of densification [*Sowers et al.*, 1992; *Blunier et al.*, 2004; *Kawamura*, 2000] (Figure 2). If close-off depth is correctly recorded by $\delta^{15}N$, the models overestimate Δage by up to 2 kyr during glacial times. We can recognize two possible sources of error in model estimates of Δage: the model representation of the physical mechanisms leading to firn metamorphism and bubble close-off, and the temperature and

[1]Department of Geosciences, Princeton University, Princeton, New Jersey, USA.
[2]Climate and Environmental Physics, Physics Institute, University of Bern, Bern, Switzerland.
[3]Laboratoire de Glaciologie et Géophysique de l'Environnement, CNRS, St. Martin d'Hères, France.
[4]Laboratoire des Sciences du Climat et de l'Environnement, Institut Pierre Simon Laplace, Commissariat à l'Energie Atomique, CNRS, Université de Versailles Saint-Quentin-en-Yvelines, Gif-sur-Yvette, France.

0148-0227/06/2005JD006488$09.00

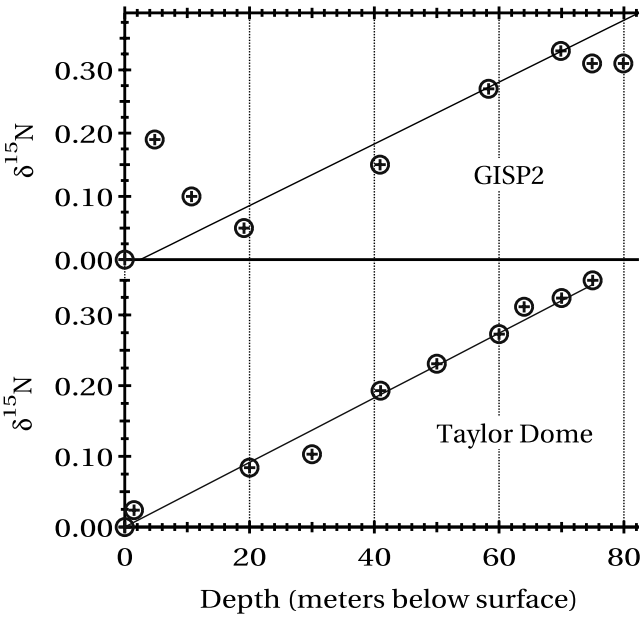

Figure 1. Firn air δ^{15}N profiles from GISP2 and Taylor Dome. The solid lines show the expected increase calculated using the barometric equation (equation (1)). The line on the GISP plot, drawn through the two deepest points in the diffusive zone (57 and 70 m), extrapolates to zero δ^{15}N at 2 m depth, indicating a convective zone of this thickness. The δ^{15}N values are reported in per mil. Analytical errors are smaller than the symbols.

accumulation histories used to drive the models. Resolving the discrepancy between the model and empirical estimates of Δage is important for accurately characterizing phasing of climate changes in different geographic regions, as well as for determining the phasing of climate events recorded in the gas and ice of a single core (e.g., deglacial CO_2 rise and East Antarctica warming). With the advent of a magnificent new ice core record from East Antarctica extending back to about 800 ka [*EPICA*, 2004], resolving this problem has become particularly important.

[4] Models of firn densification and close-off either are completely empirical [e.g., *Herron and Langway*, 1980] or are mechanistic but tuned to/validated by observations [e.g., *Arnaud et al.*, 2000]. In principle, one could test the applicability of these models to conditions of the last ice age on East Antarctica by examining densification at modern sites with extremely low temperatures and accumulation rates characteristic of glacial periods. However, no such modern sites have been studied. In the absence of such data, there are two contradictory lines of evidence bearing on the question of whether the densification models or δ^{15}N of N_2 gives a more accurate estimate of close-off age. Studies of δ^{15}N of N_2 in firn air, summarized below, show that shallow convection is minimal at most modern sites: today, therefore, δ^{15}N generally gives an accurate measure of the close-off depth. On the other hand, densification models capture the compelling systematic increase in close-off depth as temperatures fall [e.g., *Herron and Langway*, 1980]. One expects that this trend will continue such that the close-off depth will deepen during glacial times rather than become shallower. Further support for the densification models comes from the work of *Caillon et al.* [2003], who showed that these models successfully predict depths where gravitational enrichments would begin changing during glacial termination 3 at Vostok, if the convective zone thickness were monotonically related to surface temperature.

[5] In this paper we first present two new firn air profiles. We use these results, together with data from the literature, to assess the extent of shallow convection. Shallow convection would diminish the δ^{15}N enrichment, which is manifested only where convection is absent and molecular diffusion can establish isotopic gradients, but would not change the close-off depth. In addition, we recorrelate the gas records of the Greenland Ice Sheet Project 2 (GISP2) and Vostok ice cores. This correlation uses 17 control depths, based on the δ^{18}O of O_2 or the methane concentration, at which the gas age of Vostok is taken to be the same as the gas age of GISP2. We then derive three Vostok ice chronologies by calculating ice ages at the control points from gas age–ice age differences computed in three recent

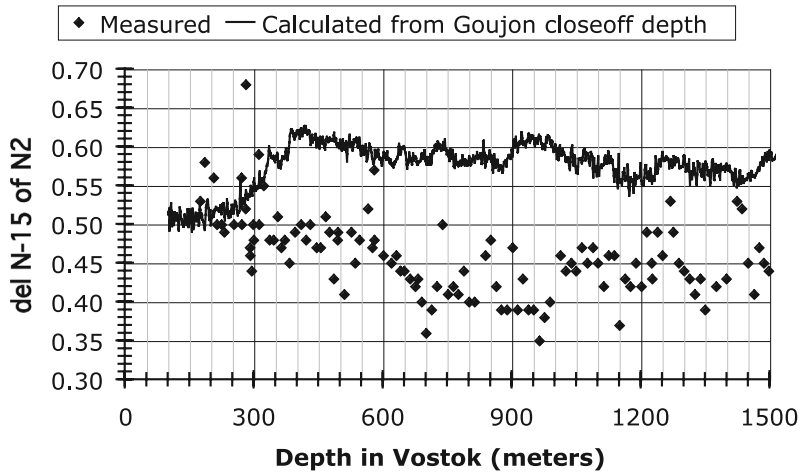

Figure 2. The δ^{15}N of N_2 (per mil) versus depth in Vostok as predicted by a glaciological model [*Goujon et al.*, 2003] and as measured.

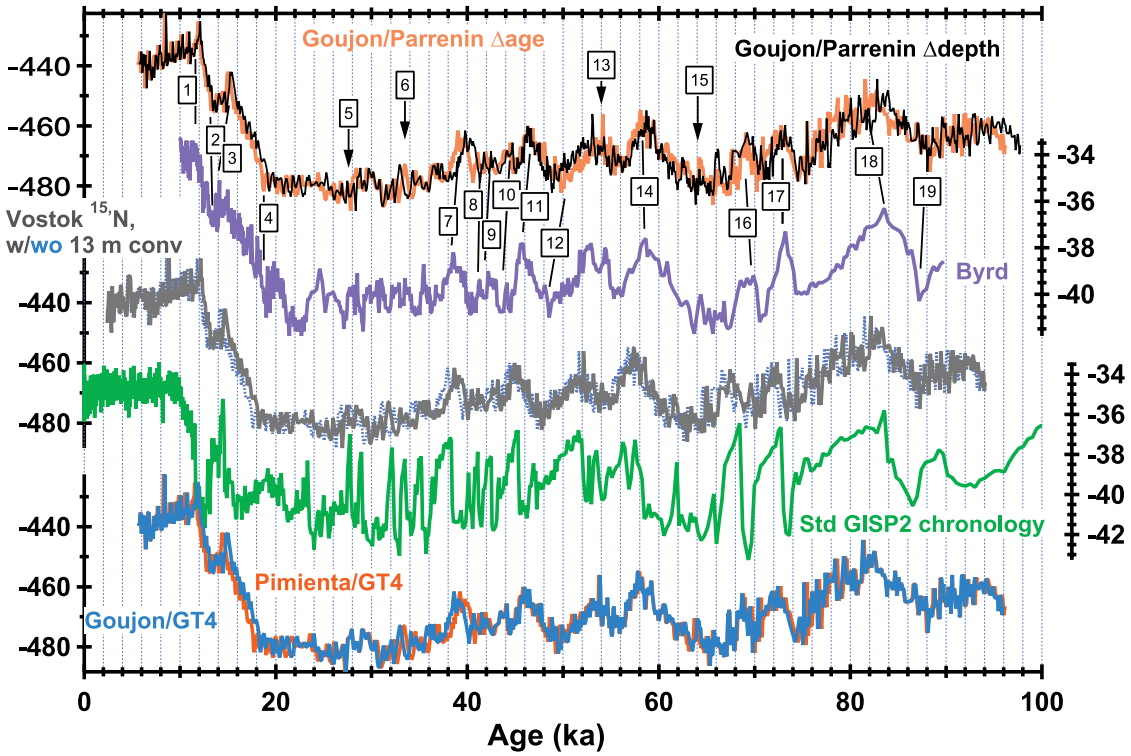

Figure 3. The $\delta^{18}O_{ice}$ (per mil) for Byrd, $\delta^{18}O_{ice}$ for GISP2, and δD (per mil) for Vostok plotted versus age. The GISP2 chronology is the standard Meese-Sowers chronology [*Meese et al.*, 1997], and the Byrd chronology is derived by correlation to GISP2 using the CH_4 stratigraphy [*Brook et al.*, 1999; *Blunier and Brook*, 2001]. The Vostok chronologies are derived as explained in the text and in Table 3. The Vostok chronologies plotted here include the CH_4 control point at 719 m depth and exclude the $\delta^{18}O_{atm}$ control point at 778 m depth. The vertical axes on the left-hand side are Vostok δD values of ice in per mil; the vertical axes on the right-hand side are GISP2 and Byrd $\delta^{18}O$ values of ice in per mil.

studies. We assign ice ages between control points assuming that relative accumulation rates in each interval vary according to the Vostok GT4 chronology [*Petit et al.*, 1999]. We also present a new approach to calculating correlation chronologies based on the correlation of control depths. This approach starts by estimating the close-off depth at each gas control depth either from $\delta^{15}N$ of N_2, or from a densification model. For each gas control depth, we calculate the depth of contemporaneous ice, on the basis of the calculated close-off depth, the average density of the firn column, and the degree to which ice has been thinned at the control depth. Again, we interpolate between ice age control points on the basis of the relative accumulation rates of the GT4 chronology.

[6] We evaluate these approaches by identifying 19 depths in the Vostok ice core marked by distinctive climate events (Figure 3). Of these 19 points, we identify 15 at which common features appear to be present in the isotopic temperature records of the Vostok and Byrd ice cores. For each Vostok chronology we calculate the mean and standard deviation between ages of temperature features recorded in the two cores. Byrd, with small, well-constrained gas age–ice age differences, has been well correlated to GISP2, and we take its chronology as a reference [*Blunier and Brook*, 2001]. The degree of agreement with Byrd indicates the accuracy with which each approach constrains the gas age–ice age difference or close-off depth. In this approach, we are implicitly assuming that gas age–ice age differences at Byrd are correctly calculated. Two facts justify this assumption. First, Δage values at Byrd are modest (<1.5 kyr), and are unlikely to have large errors. Second, glacial conditions at Byrd fall within the range of temperatures and accumulation rates at which current day close-off has been characterized.

2. Firn Air Studies

[7] Studies of the composition of air in polar firn were pioneered by *Schwander et al.* [1993]. Samples are acquired by drilling a hole to the shallowest sampling depth, sealing the bottom of the hole by lowering a long rubber bladder and inflating it against the sides, and pumping air through nylon tubing inside the bladder to sampling flasks at the surface [*Schwander et al.*, 1993]. We sampled firn air at GISP2 (72°36′N, 38°30′W) and Taylor Dome (77°47.78′N, 158°43.43′E, 2365 m elevation) using the method of Schwander et al. as modified by *Battle et al.* [1996]. GISP2 is located at the Summit site, central Greenland. Taylor Dome is located in the Dry Valleys region, Antarctica. In Figure 1, $\delta^{15}N$ of N_2 is plotted versus depth for these two previously unpublished firn air profiles.

[8] The $\delta^{15}N$ data allow one to define three zones of the firn, characterized by different modes of transport [*Sowers et al.*, 1992]. The shallowest is the convective zone, where

air is rapidly mixed by convection, and chemical and isotopic gradients are absent. Below is the diffusive zone, where convection is absent and gas transport proceeds only by atomic/molecular diffusion. In this zone, heavier gases and isotopes are enriched according to the barometric equation [*Craig et al.*, 1988; *Schwander*, 1989]. For δ^{15}N,

$$\delta^{15}\mathrm{N} = \left[e^{\Delta mgz/RT} - 1\right] * 1000, \quad (1)$$

where Δm is the mass difference between ^{15}N and ^{14}N (0.001 kg mole^{-1}), g = 9.80 m s^{-2}, z = depth (meters), R = 8.314 J mol^{-1} K^{-1}, and T = temperature (Kelvin). The solid lines in Figure 1 show values calculated from this equation. Below the diffusive zone lies the lock-in zone. Here, alternating layers of open and closed ice preserve some open porosity. Concentrations (or isotopic compositions) remain constant within individual layers, but open porosity allows firn air sampling. The depth where all porosity is closed corresponds to the bottom of the lock-in zone.

[9] Figure 1 shows the expected δ^{15}N increase with depth in the nondiffusive zone (clearest at Taylor Dome), and constant values in the lock-in zone (clearest at GISP2). GISP2 shows a shallow maximum in the upper 10 m, followed by a minimum around 20 m depth. This pattern reflects thermal fractionation, in which heavy isotopes are concentrated at the cold end of the temperature gradient in the firn that results from warm surface temperatures during the summertime sampling periods [*Severinghaus et al.*, 2001]. Because of seasonal thermal effects, the thickness of the convective zone is best diagnosed by fitting a line with the theoretical slope through the points in the non-diffusive zone (the slope, δ^{15}N/dz, is calculated from equation (1)). The thickness of the convection zone is then the x-axis intercept of this line. The derived value depends on the choice of data points. For GISP2, it is ~2 m, and for Taylor Dome, ~0, according to the lines in the figure.

[10] Thin or zero convection zones have been diagnosed at most other firn air study sites. On the basis of δ^{15}N, the convection zone was deduced to be 2–4 m at H72 [*Kawamura*, 2000], 4 m at Law Dome [*Trudinger et al.*, 2002], ~5 m at Tunu (Greenland) and Siple Dome [*Butler et al.*, 1999], and zero at South Pole [*Battle et al.*, 1996]. In addition, recent studies also using δ^{15}N find shallow convection zones at Dome C (2 m), BAS Depot in Dronning Maud Land (<5 m), Berkner Island (2 m) [*Landais et al.*, 2006], and North GRIP (1 m) [*Kawamura et al.*, 2006]. Thus convection is clearly minimal at most sites, and δ^{15}N of trapped gases faithfully records the depth of gas lock-in.

[11] Four sites are important exceptions to this generalization, and three are located in the region of slow accumulation on the East Antarctic Plateau. The δ^{15}N profiles show that the convective zone is 13 m thick at Vostok [*Bender et al.*, 1994], 8–10 m thick at Dome Fuji [*Kawamura*, 2000], and ~20 m thick at the Megadunes site [*Severinghaus et al.*, 2004]. Although the convective zone is small at Dome C [*Landais et al.*, 2006], it appears that the slow rates of accumulation and extremely cold temperatures of the East Antarctic Plateau may be conducive to thick convective zones. A surprise is the rapidly accumulating Antarctic site YM85, where the convection zone extends to 11 m [*Kawamura et al.*, 2006]. It is plausible that convection would have been deeper during the last ice age, when temperatures were colder and accumulation was lower. Nevertheless, it is difficult to imagine convection down to 40 m below surface [*Caillon et al.*, 2003; *Blunier et al.*, 2004], as is required to reconcile δ^{15}N and densification estimates of the close-off depth.

3. Comparing Ice Core Paleotemperature Records of GISP2, Byrd, and Vostok Back to 100 ka

3.1. CH_4 Studies on Vostok Ice Core Samples

[12] To improve the correlation of the Vostok and GISP2 gas records, we report here 103 new CH_4 concentration measurements made on the Vostok core by the Laboratoire de Glaciologie et Geophysique de l'Environnement. CH_4 measurements were made by the method of *Chappellaz et al.* [1997] using an automated extraction line allowing analysis of 11 samples at a time. The line has a lower blank correction than the manual extraction line, 11.6 ± 5.0 ppb. The overall analytical uncertainty (blank + chromatography) is ±10 ppb (1σ). Results are summarized in Table 1. The samples, from 845 to 1180 m depth, span the age range from about 50 to 80 ka, and greatly improve the correlation of Vostok and GISP2 in this time frame.

3.2. Correlating the Vostok and GISP2 Gas Records

[13] We use the correlations of the Vostok gas record to GISP2 based on CH_4 [*Blunier et al.*, 1998; *Blunier and Brook*, 2001] and δ^{18}O of O_2 [*Bender et al.*, 1999] to derive gas chronologies for Vostok. Control points for CH_4 are based on published data [*Brook et al.*, 1996; *Blunier and Brook*, 2001; *Petit et al.*, 1999; *Delmotte et al.*, 2004] supplemented by new results reported here (Table 1). Gas age correlation points between Vostok and GISP2 (Figure 4), derived from these CH_4 records, are listed in Table 2. The $\delta^{18}O_{atm}$ correlation points, also listed in Table 2, are as given by *Bender et al.* [1999] with one exception. The $\delta^{18}O_{atm}$ control point at 47.6 ka (788 m depth at Vostok) represents only a small minimum, and is therefore highly uncertain. It is incompatible with the new CH_4 control point at 719 m depth (45.7 ka), and is eliminated.

[14] We then use these gas chronologies to derive 6 ice chronologies for Vostok (Table 3). For each chronology we calculate an ice control point corresponding to each gas control point. We then derive a continuous timescale by interpolating between ice control points on the basis of the relative age-depth scale of the GT4 chronology [*Petit et al.*, 1999].

[15] We derive three chronologies using the traditional approach of calculating Δage (gas age–ice age difference) for each control points (Table 4). The first of these (Pimienta/GT4) is simply based on the GT4 ice chronology [*Petit et al.*, 1999] and the firn densification model of *Pimienta* [1987] that was used to generate the original GT4 gas chronology. The two inputs to this model are firn temperature and accumulation rate; both properties are estimated from δD of the ice, which constrains surface temperature. The second chronology (Goujon/GT4) is based on the GT4 timescale, the semimechanistic firn densification model of *Arnaud et al.* [2000], and a thermal model of the firn [*Goujon et al.*, 2003]. Firn temperatures are relevant because they influence the rate of snow metamorphism and,

Table 1. CH_4 Concentrations in Newly Analyzed Samples From the Vostok Ice Core

Depth in Vostok	CH_4, ppb
845.50	420.1
848.88	414.8
851.18	434.7
854.35	476.4
857.19	507.2
860.37	481.7
863.04	497.0
866.55	455.5
869.17	459.6
872.77	459.6
875.18	503.3
878.29	520.1
881.18	556.1
884.04	549.7
887.16	522.9
890.03	532.4
900.70	508.0
908.49	513.6
911.18	484.0
914.30	458.2
917.18	422.1
921.23	423.8
923.15	448.7
926.33	448.2
929.57	412.7
932.13	422.7
937.19	428.9
940.66	449.8
943.44	422.1
946.70	433.4
949.34	416.4
952.18	414.4
956.17	430.9
958.33	423.0
961.97	411.0
964.66	417.7
967.03	421.5
970.18	424.8
973.18	426.7
976.18	436.4
979.03	451.4
982.58	449.1
984.03	465.0
987.68	425.6
990.67	422.5
993.19	418.8
996.17	434.2
999.65	435.3
1002.03	448.9
1005.03	437.7
1008.52	443.9
1011.18	446.2
1013.35	446.3
1016.15	439.1
1019.29	450.6
1022.57	470.9
1025.53	434.9
1028.13	432.5
1031.35	438.4
1033.03	454.2
1037.46	444.2
1040.19	453.6
1043.32	449.8
1046.03	462.7
1048.33	443.5
1051.58	448.2
1055.12	430.2
1057.66	457.2
1060.71	448.9
1063.03	449.7
1066.03	452.5
1070.03	450.6
1072.18	465.2
1075.18	464.1
1078.28	432.5
1081.17	426.9
1085.53	424.3
1087.33	419.6
1090.28	424.4
1093.18	436.0
1096.67	433.8
1099.63	426.8
1102.17	440.5
1104.63	443.2
1108.27	435.0
1111.03	435.0
1114.47	444.3
1117.17	447.0
1120.85	455.2
1123.12	444.3
1126.17	457.4
1132.03	449.6
1135.03	391.4
1138.18	401.9
1141.26	425.0
1159.68	448.6
1162.19	457.6
1165.56	460.1
1168.34	437.0
1171.16	467.1
1174.64	471.1
1177.22	476.8
1180.68	491.9

hence, the close-off depth. The third chronology (Goujon/Parrenin Δage) differs from the second in that it is based on the ice chronology of *Parrenin et al.* [2004]. These authors modify the GT4 chronology by improving the thinning function of ice in the context of the upstream flow, and by decreasing the glacial accumulation rates. Both changes lead to important revisions in the chronologies. For each chronology, we calculate Δage at each gas age control depth to get an ice age at that depth. We then interpolate ages between control depths adopting the relative accumulation rates of the GT4 chronology.

[16] The GT4 chronology is based on a model of ice flow tuned to give ages consistent with deep sea sediment chronologies at depths of 1534 m (110 ka) and 3254 m (390 ka). The Pimienta densification model invokes empirical relationships between density, close-off depth, and mean annual temperature and accumulation. The firn model of *Arnaud et al.* [2000] interprets the empirical data in terms of mechanistic equations describing grain growth and densification. The thermal model of *Goujon et al.* [2003] recognizes the role of geothermal heat in warming firn and promoting densification. Finally, the ice flow model of *Parrenin et al.* [2004] takes into account the thickness of ice and the nature of basal topography along the flow path when evaluating how ice at Vostok is thinned with depth and age.

[17] We derive three additional chronologies using a new approach in which we calculate Δdepth (the current depth difference between a gas control point and its correlative ice depth). In each case, we adopt a value of 0.7 for the ratio of the height of the fully compacted ice column (density =

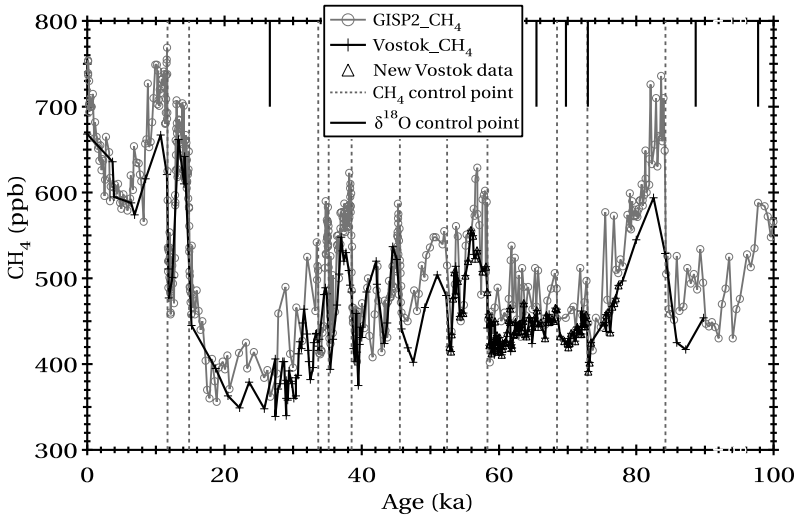

Figure 4. CH_4 records for GISP2 and Vostok versus age. Vertical lines indicate gas age correlation points based on CH_4. CH_4 concentrations are in units of ppb.

0.91 gm cm^{-3}) to the original uncompacted firn, from the surface to the close-off depth. This value of 0.7 is typical of modern conditions on the East Antarctic Plateau [e.g., *Herron and Langway*, 1980]. This compacting factor changes by no more than 5% for conditions in the past [*Blunier et al.*, 2004]. The first Δdepth chronology ($\delta^{15}N$) is based on $\delta^{15}N$ of N_2, previously measured in Vostok (available from the National Snow and Ice Data Center). The $\delta^{15}N$ values are corrected for thermal diffusion so that they represent the result of gravitational fractionation alone (the magnitude of this correction is order 0.02‰). Surface temperature is taken from *Petit et al.* [1999]. The temperature gradient in the firn, which influences $\delta^{15}N$ because of thermal fractionation [*Severinghaus et al.*, 2001], is calculated by a newly constructed thermal model similar to that of *Goujon et al.* [2003]. The original close-off depth is calculated from $\delta^{15}N$ according to equation (1), given the surface temperature record inferred from δD of the ice. The current Δdepth value is calculated from the close-off depth, the compaction factor (0.7), and the thinning function [*Parrenin et al.*, 2004]. The second Δdepth chronology ($\delta^{15}N$ + 13 m) is identical, except there is assumed to be a convective zone of 13 m, the current condition at Vostok [*Bender et al.*, 1994]. The third Δdepth chronology (Goujon/Parrenin Δdepth) calculates the close-off depth from the densification model of *Arnaud et al.* [2000], the firn thermal model of *Goujon et al.* [2003], and the ice chronology (including thinning function) of *Parrenin et al.* [2004].

[18] The Goujon/Parrenin Δage chronology invokes the same gas control ages and gas trapping depths as the Goujon/Parrenin Δdepth chronology. These ice chronologies differ, however, because they use different approaches for deriving ice ages from each of the gas age control points. The Δage chronology adds Δage to calculate an ice age for each gas age control point. Δage depends on accumulation rate, which may be poorly known and therefore introduces considerable uncertainty. The Δdepth chronology subtracts the densified and thinned firn column from a gas depth to get the correlative ice depth. The degree of densification is well known and, at shallow depths, the thinning is generally small and accurately characterized. Deep in the core, however, thinning is extensive and less accurately known.

[19] Vostok ice originates along the Ridge B/Vostok ice flow line, and past variations in the ice thickness along this flow line affect the thinning function of ice that is now at the Vostok site. In the section of the Vostok core of interest here (last 100 ka), the thinning function varies between 0.8 and 1.0, and has recently been improved by taking into account bedrock topography upstream of Vostok [*Parrenin et al.*, 2004]. Still, there remain sources of uncertainty in this modeled thinning function. First, *Parrenin et al.* [2004] did not take into account the temporal variations in ice thickness, which have a significant impact on the thinning function. Second, *Parrenin et al.* [2004] assumed a path for the flow above Lake Vostok that does not coincide exactly with the path induced by examining isochronous layers [*Tikku et al.*, 2004]. Third, it is not clear that the trajectory of the ice flow line has been stable in the past. Fourth, a mechanical model that is more complex than used by *Parrenin et al.* [2004], and that takes into account the different mechanical properties of the ice from different

Table 2. Control Points for Correlating Vostok and GISP2 Gas Chronologies

Source	GISP2 Depth, m	Vostok Depth, m	GISP2 Gas Age, ka
GT4		150.00	2.36
CH_4	1699	323.10	11.73
CH_4	1818.5	374.00	14.84
$\delta^{18}O_{atm}$	2047.00	498.00	26.60
CH_4	2161.00	581.80	33.67
CH_4	2190.00	596.45	35.17
CH_4	2244.00	629.20	38.52
CH_4	2370.00	718.85	45.55
CH_4	2461.00	840.15	52.43
CH_4	2512.00	911.18	58.32
$\delta^{18}O_{atm}$	2566.00	1046.00	65.45
CH_4	2587.00	1076.73	68.44
$\delta^{18}O_{atm}$	2594.00	1082.00	69.74
$\delta^{18}O_{atm}$	2617.00	1133.50	72.94
CH_4	2679.00	1261.20	84.24
$\delta^{18}O_{atm}$	2699.00	1327.00	88.65
$\delta^{18}O_{atm}$	2736.00	1422.00	97.75

Table 3. Models Used To Calculate Ice Ages From Gas Ages

Model	Characteristics
Models Calculated by Deriving Ice Ages at Depths of Gas Age Control Points	
Pimienta/GT4	GT4 temperature, accumulation rate, thinning function [*Petit et al.*, 1999]; *Pimienta* [1987] close-off model
Goujon/GT4	GT4 chronology; *Arnaud et al.* [2000] close-off model taking into effect firn temperature as calculated with the thermal model of *Goujon et al.* [2003]
Goujon/Parrenin Δage	same as Goujon/GT4 but calculated with the thinning function of *Parrenin et al.* [2004]
Models Calculated by Deriving Ice Depths of Gas Age Control Points	
δ^{15}N	close-off depth calculated from δ^{15}N of N_2 assuming no convective zone
δ^{15}N + 13 m	same as δ^{15}N, except that we assume a 13 m convective zone at the top of the firn
Goujon/Parrenin Δdepth	close-off depth calculated as in Goujon/Parrenin model; current gas-ice depth difference calculated from *Parrenin et al.* [2004] thinning function

time periods, might give different results. In total, we estimate that the uncertainty in the thinning function may not be better than ±0.1 for the upper ~1500 m of the Vostok core that is relevant to this paper. In general, the Δage method may be preferable for the lower part of an ice core (where the ice is more thinned and the relative uncertainty in thinning function is higher), and the Δdepth approach may be better for the shallower part, where there is less thinning and use of the thinning function introduces less uncertainty.

3.3. Intercomparison of Chronologies

[20] For the purpose of evaluating our 6 chronologies, we define 19 depths in the Vostok core marked by local maxima or minima in δD (Figure 3). Seventeen of these extrema correspond to events of the same direction and approximate age in the Byrd core (previously correlated to GISP2 by detailed CH_4 stratigraphy) [*Blunier and Brook*, 2001], and we assume these events are synchronous. For each correlative event, we calculate the Vostok-Byrd age difference according to each of our Vostok chronologies

Table 4. Ages of Gas and Ice Control Points[a]

Vostok Depth, m	Vostok Correlation Gas Age, ka	Vostok Ice Age, Pimienta/GT4, ka	Vostok Ice Age, Goujon/GT4, ka	Vostok Ice Age, Goujon/Parrenin ΔAge, ka
150.00	2.36	5.68	5.66	5.59
323.10	11.73	15.30	15.81	15.96
374.00	14.84	19.36	20.09	20.54
498.00	26.60	33.35	32.93	33.44
581.80	33.67	40.03	39.37	39.78
596.45	35.17	41.29	40.75	41.14
629.20	38.52	43.83	43.92	44.27
718.85	45.55	50.63	50.94	51.24
840.15	52.43	57.70	57.54	57.82
911.18	58.32	63.22	63.55	63.75
1046.00	65.45	70.85	70.55	71.01
1076.73	68.44	73.63	73.37	73.68
1082.00	69.74	75.00	74.66	75.02
1133.50	72.94	77.90	77.65	77.93
1261.20	84.24	88.52	88.68	88.88
1327.00	88.65	93.09	92.93	93.17
1422.00	97.75	101.98	101.75	101.93
Vostok Correlation Depth, m	**Vostok Correlation Gas Age, ka**	**Vostok Ice Depth δ^{15}N, m**	**Vostok Ice Depth δ^{15}N + 13 m, m**	**Vostok Ice Depth, Goujon/Parrenin ΔDepth, m**
150.00	2.36	75.5	75.5	86.1
323.10	11.73	261.1	253.4	256.2
374.00	14.84	322.1	313.8	303.3
498.00	26.60	447.7	440.2	424.3
581.80	33.67	528.9	520.2	507.5
596.45	35.17	545.0	535.9	521.9
629.20	38.52	576.8	568.5	554.3
718.85	45.55	673.1	665.0	642.6
840.15	52.43	785.8	777.2	765.0
911.18	58.32	866.3	857.6	835.8
1046.00	65.45	996.7	989.2	974.0
1076.73	68.44	1027.3	1018.7	1005.3
1082.00	69.74	1035.5	1026.9	1010.5
1133.50	72.94	1084.3	1076.0	1063.9
1261.20	84.24	1209.8	1202.0	1195.4
1327.00	88.65	1286.4	1279.2	1264.8
1422.00	97.75			1364.7

[a]Upper part of table shows chronologies based on gas age–ice age differences. Bottom part of table shows chronologies based on gas depth–ice depth differences. Ages are in ka (thousands of years before present).

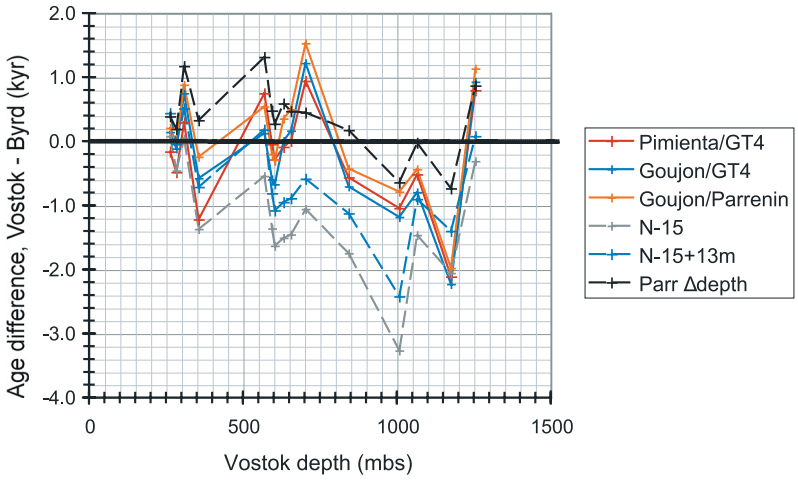

Figure 5. Vostok-Byrd age differences at comparison points for the various chronologies. Pimienta/GT4 refers to the original chronology of *Petit et al.* [1999]. Other chronologies are summarized in Table 3.

(Figure 5 and Table 5). The differences, ideally zero, give a measure of the validity of the respective chronologies and the approaches used to derive them. They also give a useful way to intercompare the various Vostok chronologies.

[21] We start by intercomparing the three Vostok chronologies in which gas age–ice age differences are calculated from glaciological models. Ages of Vostok events calculated with the Goujon Δage values (Goujon/GT4) are, on average, slightly younger than ages calculated with Δage values from the densification model of *Pimienta* [1987], used in the GT4 chronology of *Petit et al.* [1999] (Pimienta/GT4). The values can differ by up to 0.8 kyr at specific depths in the core. These differences of course reflect the different approaches used to calculate Δage. These variations are reflected in the Vostok-Byrd age differences calculated for the two chronologies. On average, there is very little difference in ages calculated using the GT4 close-off depths and those of Pimienta or Goujon. Ages calculated with the close-off depths (and accumulation rates) of Parrenin (Parrenin/Goujon) are older on average by 0.3–0.4 kyr. The Vostok-Byrd comparison does not identify any of these three chronologies as superior. Parrenin/Goujon ages are older than Byrd by 0.1–0.2 kyr, while the other two chronologies are younger by 0.1–0.3 kyr (depending on which chronology and whether one excludes the comparison for event 18, which is poorly dated to ±0.8 kyr in Byrd). The standard deviations of Vostok-Byrd differences are similar, falling in the range of ±0.7–0.9 kyr.

[22] We next intercompare the three Vostok chronologies derived on the basis of Δdepth differences. Calculating Δdepth from the glaciological model (Goujon/Parrenin Δdepth), rather than δ^{15}N (no convection zone), increases ice age by 1.5–1.6 kyr. Compared with Byrd, ages of correlative events are 1.2 kyr older in Vostok when calculated using δ^{15}N and assuming no convective layer. This is the largest mean age difference between any Vostok chronology and Byrd, and we accordingly reject δ^{15}N alone as the basis for calculating Δage. Vostok ages are 0.6 kyr younger than Byrd when Δdepth is calculated using δ^{15}N and a 13 m convection depth, and 0.4 kyr older when calculated using the Δdepth derived from the glaciological model (Goujon/Parrenin Δdepth). Age differences show less variance with the glaciological Δdepth values (±0.5–0.6 kyr) than with any other model.

[23] On the basis of this comparison, we believe that the methods of choice for transferring gas to ice chronologies are the Goujon/Parrenin Δage model and the Goujon/Parrenin Δdepth model. Both invoke the glaciological model of *Arnaud et al.* [2000], the firn air temperature model of *Goujon et al.* [2003], and an appropriate chronology (that of *Parrenin et al.* [2004] in the case of Vostok). The Goujon/Parrenin Δage model includes more physical processes than Pimienta/GT4 or Goujon/GT4.

[24] With respect to the approaches using δ^{15}N, we judge the one based on δ^{15}N alone as unsatisfactory, because it gives a much larger difference between ages of Vostok and Byrd events than any other chronology. We downgrade the Δdepth approach based on δ^{15}N and a 13 m convection zone because there is no reason to believe that the modern convection zone thickness has always prevailed. Our results imply that the convection zones at sites of deep East Antarctic ice cores were indeed consistently of order 40 m during glacial times, as required to rationalize the difference between δ^{15}N values and close-off depths estimated by glaciological models [e.g., *Sowers et al.*, 1992].

[25] The underlying physics is similar for our two selected chronologies: each invokes the same glaciological model, thermal model, and chronology (including thinning function). However, as noted above, the chronology derived for the Δage approach is different from that for the Δdepth approach. The reason is that Δage depends strongly on accumulation rate and is independent of the thinning function, while Δdepth is only weakly dependent on accumulation rate but depends strongly on the thinning function. These distinctions lead to significantly different chronologies. The Δage chronology is preferable when accumulation rate is better constrained than the thinning function, whereas the Δdepth chronology is preferable when thinning rate is better constrained.

[26] Finally, we note that there are sometimes systematic changes among all chronologies in Vostok-Byrd age differences for some events. For example, for all chronologies,

Table 5. Summary of Vostok Ages and Vostok-Byrd Age Differences for Vostok-Byrd Comparison Points[a]

Event	Vostok Depth	Goujon/Parrenin Δage	^{15}N	^{15}N + 13 m	Pimienta/GT4	Goujon/GT4	Goujon/Parrenin Δdepth
			Ages of Events at Vostok According to Chronology				
1	263	11.9	11.8	12.2	11.6	11.9	12.1
2	284	13.3	12.8	13.2	12.8	13.2	13.5
3	309	15.0	14.2	14.6	14.4	14.9	15.3
4	356	18.8	17.6	18.3	17.8	18.4	19.3
5	444	27.8	26.3	27.0	27.3	27.3	28.3
6	498	33.4	31.0	31.7	33.4	32.9	32.9
7	570	39.0	37.9	38.7	39.2	38.6	39.8
8	595	41.1	39.9	40.4	41.2	40.7	41.7
9	604	41.9	40.6	41.1	41.9	41.5	42.5
10	632	44.5	42.6	43.2	44.0	44.1	44.7
11	656	46.3	44.4	44.9	45.8	46.0	46.3
12	704	50.1	47.5	48.0	49.5	49.8	49.0
13	772	54.1	51.7	52.1	53.7	53.8	53.1
14	844	58.1	56.8	57.4	58.0	57.8	58.7
15	920	64.2	61.2	61.6	63.7	64.0	62.5
16	1008	69.1	66.6	67.4	68.8	68.7	69.2
17	1066	72.8	71.8	72.3	72.7	72.4	73.2
18	1176	81.6	81.5	82.1	81.4	81.3	82.8
19	1255	88.3	86.9	87.3	88.0	88.1	88.0
			Age Differences, Vostok-Byrd, kyr				
1	263	0.2	0.1	0.4	−0.2	0.1	0.4
2	284	0.0	−0.5	0.0	−0.5	−0.1	0.2
3	309	0.9	0.0	0.5	0.3	0.7	1.2
4	356	−0.2	−1.4	−0.7	−1.2	−0.6	0.3
7	570	0.5	−0.5	0.2	0.7	0.1	1.3
8	595	−0.2	−1.4	−0.8	0.0	−0.6	0.5
9	604	−0.3	−1.6	−1.1	−0.3	−0.7	0.3
10	632	0.4	−1.5	−0.9	−0.1	0.0	0.6
11	656	0.5	−1.5	−0.9	0.0	0.2	0.5
12	704	1.5	−1.1	−0.6	0.9	1.2	0.4
14	844	−0.4	−1.8	−1.1	−0.6	−0.7	0.2
16	1008	−0.8	−3.3	−2.4	−1.0	−1.2	−0.6
17	1066	−0.4	−1.5	−0.9	−0.5	−0.8	0.0
18	1176	−2.0	−2.1	−1.4	−2.1	−2.2	−0.7
19	1255	1.1	−0.3	0.1	0.8	0.9	0.9
			All Samples				
Average deviation, kyr		0.1	−1.2	−0.6	−0.3	−0.2	0.4
SD of deviation, kyr		0.9	0.9	0.8	0.8	0.9	0.6
RMS of deviation, kyr		0.9	1.5	1.0	0.9	0.9	0.7
			Excluding Event 18				
Average deviation, kyr		0.2	−1.1	−0.6	−0.1	−0.1	0.4
SD of deviation, kyr		0.7	0.9	0.8	0.7	0.7	0.5
RMS of deviation, kyr		0.7	1.5	1.0	0.7	0.7	0.7

[a]Ages are in ka (thousands of years before present), and age differences are in kyr. Depths are in meters. SD, standard deviation; RMS, root-mean-square.

the age difference between Vostok and Byrd is greater for event 3 than for events 2 and 4. Such systematic differences could be due to errors in correlations of the isotopic temperature records between Byrd and Vostok, to errors in the gas age control points established between Vostok, Byrd, and GISP2, or to errors in the interpolations between gas age control points. These uncertainties represent fundamental limitations to our approach and prevent us from validating a delta age method to better than about ±1.0 kyr.

4. Summary and Conclusions

[27] We have presented two new firn air profiles of $\delta^{15}N$ of N_2, and used these results, together with data in the literature, to assess the likelihood for deep convection in the firn that would attenuate the normal gravitational enrichments. The 103 new analyses of CH_4 in the Vostok ice core, together with existing data from the literature, lead to a new Vostok timescale for the gas records that is more accurately correlated with GISP2.

[28] Ice chronologies, calculated from gas chronologies on the basis of different assumptions, lead to ages for Vostok climate events that can be compared with ages of correlative events in the Byrd core. We conclude that $\delta^{15}N$ seriously underestimates the close-off depth of glacial Vostok ice, presumably because of deep convection. *Kawamura and Severinghaus* [2005] recently discovered that, at the Megadunes Site, Antarctica, low $\delta^{15}N$ values are associated with deep cracks in the ice. Their result lends plausibility to our conclusion and suggests a mechanism for deep convection. Our leading chronologies are both based on the *Arnaud et al.* [2000] firn densification model, calculated values of temperature versus depth in the firn [*Goujon et al.*, 2003], and the Vostok accumulation rate or thinning function

of *Parrenin et al.* [2004]. The uncertainty in the Vostok gas age–ice age difference is still ~1 kyr, complicating an accurate assessment of climate phasing between Greenland and East Antarctica during the last ice age. Our analysis should be repeated for deep East Antarctic ice cores drilled on domes. Uncertainties may be smaller at such sites because, relative to Vostok, the thinning function and perhaps other glaciological properties are better constrained.

[29] **Acknowledgments.** Financial support to Princeton came from the National Science Foundation, Office of Polar Programs (Antarctic Division), and the Gary Comer Family Foundation. CH_4 measurements at LGGE were supported by the EC project Pole-Ocean-Pole (EVK2-2000-22067). Additional financial support in France was provided by the Programme National d'Etudes de la Dynamique du Climat (INSU-CNRS) and the CEA. The University of Bern was supported by the Swiss National Science Foundation. We thank ice drillers and all participants in the fieldwork and ice sampling, the Russian Antarctic Expeditions (RAE), and the Institut Polaire Francais Paul Emile Victor (IPEV).

References

Arnaud, L., J.-M. Barnola, and P. Duval (2000), Physical modeling of the densification of snow/firn and ice in the upper part of ice sheets, in *Physics of Ice Core Records*, edited by T. Hondoh, pp. 285–305, Hokkaido Univ. Press, Sapporo, Japan.

Battle, M., M. Bender, T. Sowers, P. P. Tans, J. H. Butler, J. W. Elkins, J. T. Ellis, T. Conway, N. Zhang, P. Lang, and A. D. Clarke (1996), Atmospheric gas concentrations over the past century in air from firn at the South Pole, *Nature*, *383*, 231–235.

Bender, M. L., T. Sowers, J.-M. Barnola, and J. Chappellaz (1994), Changes in the O_2/N_2 ratio of the atmosphere during recent decades reflected in the composition of air in the firn at Vostok Station, Antarctica, *Geophys. Res. Lett.*, *21*, 189–192.

Bender, M. L., B. Malaize, J. Orchardo, T. Sowers, and J. Jouzel (1999), High precision correlations of Greenland and Antarctica over the last 100 kyr, in *Mechanisms of Global Climate Change at Millennial Timescales*, *Geophys. Monogr. Ser.*, vol. 112, edited by P. Clark, R. Webb, and L. Keigwin, pp. 165–175, AGU, Washington, D. C.

Blunier, T., and E. J. Brook (2001), Timing of millennial-scale climate change in Antarctica and Greenland during the last glacial period, *Science*, *273*, 1087–1091.

Blunier, T., et al. (1998), Asynchrony of Antarctic and Greenland climate change during the last glacial period, *Nature*, *394*, 739–743.

Blunier, T., J. Schwander, J. Chappellaz, F. Parrenin, and J. M. Barnola (2004), What was the surface temperature in central Antarctica during the last glacial maximum?, *Earth Planet. Sci. Lett.*, *218*, 379–388.

Brook, E. J., T. Sowers, and J. Orchardo (1996), Rapid variations in atmospheric methane concentration during the past 110,000 years, *Science*, *273*, 1087–1091.

Brook, E. J., S. Harder, J. Severinghaus, and M. Bender (1999), Atmospheric methane and millennial-scale climate change, in *Mechanisms of Global Climate Change at Millennial Timescales*, *Geophys. Monogr. Ser.*, vol. 112, edited by P. Clark, R. Webb, and L. Keigwin, pp. 165–175, AGU, Washington, D. C.

Butler, J. H., et al. (1999), A record of atmospheric halocarbons during the twentieth century from polar firn air, *Nature*, *399*, 749–755.

Caillon, N., J. P. Severinghaus, J. Jouzel, J.-M. Barnola, J. C. Kang, and V. Y. Lipenkov (2003), Timing of atmospheric CO_2 and Antarctic temperature changes across termination III, *Science*, *299*, 1728–1731.

Chappellaz, J., T. Blunier, S. Kints, A. Dallenbach, J. M. Barnola, J. Schwander, D. Raynaud, and B. Stauffer (1997), Changes in the atmospheric CH_4 gradient between Greenland and Antarctica during the Holocene, *J. Geophys. Res.*, *102*, 15,987–15,997.

Craig, H., Y. Horibe, and T. Sowers (1988), Gravitational separation of gases and isotopes in polar ice caps, *Science*, *242*, 1675–1678.

Delmotte, M., et al. (2004), Atmospheric methane during the last four glacial-interglacial cycles: Rapid changes and their link with Antarctic temperature, *J. Geophys. Res.*, *109*, D12104, doi:10.1029/2003JD004417.

EPICA Community Members (2004), Eight glacial cycles from an Antarctic ice core, *Nature*, *429*, 623–628.

Goujon, C., et al. (2003), Modeling the densification of polar firn including heat diffusion: Application to close-off characteristics and gas isotopic fractionation for Antarctica and Greenland sites, *J. Geophys. Res.*, *108*(D24), 4792, doi:10.1029/2002JD003319.

Herron, M. M., and C. C. Langway Jr. (1980), Firn densification: An empirical model, *J. Glaciol.*, *25*, 373–385.

Kawamura, K. (2000), Variations of atmospheric components over the past 340,000 years from Dome Fuji deep ice core, Antarctica, Ph.D. dissertation, Tohoku Univ., Sendai, Japan.

Kawamura, K., and J. P. Severinghaus (2005), Krypton and xenon as indicators of convective zone thickness in firn at Megadunes, Antarctica, *Eos Trans. AGU*, *86*(52), Fall Meet. Suppl., Abstract PP33C-1590.

Kawamura, K., J. P. Severinghaus, S. Ishidoya, S. Sugawara, G. Hashida, H. Motoyama, Y. Fujii, S. Aoki, and T. Nakazawa (2006), Convective mixing of air in firn at four polar sites, *Earth Planet. Sci. Lett.*, *244*, 672–682.

Landais, A., J. M. Barnola, K. Kawamura, N. Caillon, M. Delmotte, T. Van Ommen, G. Dreyfus, J. Jouzel, V. Masson-Delmotte, and B. Minster (2006), Firn-air $\delta^{15}N$ in modern polar sites and glacial-interglacial ice: A model-data mismatch during glacial periods in Antarctica?, *Quat. Sci. Rev.*, *25*, 49–62.

Meese, D., A. J. Gow, R. B. Alley, G. A. Zielinsk, P. M. Grootes, M. Ram, K. C. Taylor, P. A. Mayewski, and J. F. Bolzan (1997), The Greenland Ice Sheet Project 2 depth-age scale: Methods and results, *J. Geophys. Res.*, *102*, 26,411–26,423.

Parrenin, F., F. Remy, C. Ritz, M. J. Siegert, and J. Jouzel (2004), New modeling of the Vostok ice flow line and implication for the glaciological chronology of the Vostok ice core, *J. Geophys. Res.*, *109*, D20102, doi:10.1029/2004JD004561.

Petit, J. R., et al. (1999), Climate and atmospheric history of the past 420,000 years from the Vostok ice core, Antarctica, *Nature*, *399*, 429–436.

Pimienta, P. (1987), Etude du comportement mecanique des glaces polycristallines aux faibles contraintes: Applications aux glaces des carottes polaires, Univ. des Sci. et Technol. Med. de Grenoble, Grenoble, France.

Schwander, J. (1989), The transformation of snow to ice and the occlusion of gases, in *Environmental Record in Glaciers and Ice Sheets*, edited by H. Oeschger and C. C. Langway Jr., pp. 53–67, John Wiley, Hoboken, N. J.

Schwander, J., J.-M. Barnola, C. Andrie, M. Leuenberger, A. Ludin, D. Raynaud, and B. Stauffer (1993), The age of the air in the firn and the ice at Summit, Greenland, *J. Geophys. Res.*, *98*, 2831–2838.

Severinghaus, J. P., A. Grachev, and M. Battle (2001), Thermal fractionation of air in polar firn by seasonal temperature gradients, *Geochem. Geophys. Geosyst.*, *2*(7), doi:10.1029/2000GC000146.

Severinghaus, J. P., M. Fahnestock, M. Albert, and T. Scambos (2004), Do deep convective zones exist in low-accumulation firn?, *Eos Trans. AGU*, *84*(47), Fall Meet. Suppl., Abstract C31C-07.

Sowers, T., M. Bender, and D. Raynaud (1989), Elemental and isotopic composition of occluded O_2 and N_2 in polar ice, *J. Geophys. Res.*, *94*, 5137–5150.

Sowers, T., M. Bender, D. Raynaud, and Y. S. Korotkevitch (1992), The $\delta^{15}N$ of N_2 in air trapped in polar ice: A tracer of gas transport in the firn and a possible constraint on ice age–gas age differences, *J. Geophys. Res.*, *97*, 15,683–15,697.

Tikku, A. A., R. E. Bell, M. Studinger, and G. K. C. Clarke (2004), Ice flow field over Lake Vostok, East Antarctica inferred by structure tracking, *Earth Planet. Sci. Lett.*, *227*, 249–261.

Trudinger, C. M., et al. (2002), Reconstructing atmospheric histories from measurements of air composition in firn, *J. Geophys. Res.*, *107*(D24), 4780, doi:10.1029/2002JD002545.

J.-M. Barnola, J. Chappellaz, and F. Parrenin, Laboratoire de Glaciologie et Géophysique de l'Environnement (LGGE), CNRS, BP 96, F-38402 St. Martin d'Hères Cedex, France.

M. L. Bender and M. Suwa, Department of Geosciences, Princeton University, Princeton, NJ 08540, USA. (bender@princeton.edu)

T. Blunier and G. Floch, Climate and Environmental Physics, Physics Institute, University of Bern, Sidlerstrasse 5, CH-3012 Bern, Switzerland.

G. Dreyfus and J. Jouzel, Institut Pierre Simon Laplace/Laboratoire des Sciences du Climat et de l'Environnement, CEA-CNRS-UVSQ, Bâtiment 701, CE Saclay, Orme des Merisiers, F-91191 Gif-sur-Yvette, France.